Proc. 8th Int. Conf. Quarks and Nuclear Physics (QNP2018)
JPS Conf. Proc. **26**, 024007 (2019)
https://doi.org/10.7566/JPSCP.26.024007

Studying the QCD Phase Diagram in RHIC-BES at STAR

Toshihiro Nonaka for the STAR Collaboration
Central China Normal University, Wuhan 430079, China
Key Laboratory of Quark & Lepton Physics (MOE) and Institute of Particle Physics
E-mail: tnonaka@rcf.rhic.bnl.gov

(Received January 29, 2019)

The beam energy scan (BES-I) program was carried out in BNL-RHIC in order to study the QCD phase diagram. In this talk, we presented some experimental results obtained in the STAR experiment, in a view of freeze-out conditions, phase transition boundary, smooth crossover ($\mu_{\rm B} \sim 0$ MeV) and critical-end-point ($\mu_{\rm B} > 0$ MeV). Most impressive observation is the non-monotonic collision energy dependence of the 4th-order fluctuations of the net-proton multiplicity distribution. Furthermore, negative sign of the 6th-order fluctuations has been observed for net-proton distribution at the RHIC top energy.

KEYWORDS: QGP, QCD phase diagram, heavy-ion collisions, RHIC, STAR

1. Introduction

One of the main goals of the heavy-ion collision experiments is to study the QCD phase diagram with respect to the temperature (T) and the baryon chemical potential (μ_B). From the various experimental results so far, a Quark-Gluon Plasma (QGP) phase is expected to be created in high temperature and/or high baryon density region, while a hadron gas phase is expected to exist in the region of low temperature and density. Next step to understand the QCD phase structure is to study the mechanism of the phase transition between QGP and hadron gas phases. It was shown by the lattice QCD calculation that the phase transition at $\mu_B \sim 0$ MeV is a smooth crossover without clear boundary [1]. On the other hand, the phase transition is predicted to be the 1st-order at large μ_B [2,3]. If the 1st-order phase transition exists, there should be also the critical end point, which is the connecting point between crossover and the 1st-order phase transition.

In order to study the QCD phase structure experimentally, the beam energy scan (BES-I) program was carried out at Relativistic Heavy Ion Collider (RHIC) starting from 2010. The STAR experiment collected huge data sets at the collision energy of $\sqrt{s_{\rm NN}}$ =7.7, 11.5, 14.5, 19.7, 27, 39, 54.4, 62.4 and 200 GeV. In this talk, we present some results obtained in the STAR experiment related to the QCD phase structure. First, we discuss the freeze-out parameters which are the important variables to understand the dynamics in the heavy-ion collisions. Second, the results of the directed flow of the identified particles are shown in order to find the signal from the 1st-order phase transition. Third, the results on the critical point search using the higher-order fluctuations of the conserved quantities are presented. Finally, the results of the 6th-order fluctuations are discussed in search for the experimental evidence of a smooth crossover at vanishing $\mu_{\rm B}$.

2. Freeze-out conditions

There are two kinds of freeze-out in heavy-ion collisions. The first one is the chemical freeze-out, where the inelastic collisions cease. The second one is the kinetic freeze-out, where the elastic collisions cease. In order to extract the chemical freeze-out parameters, hadron yields for various particle

species have been measured and compared with the hadron resonance gas model [7]. The kinetic freeze-out parameters have been obtained by blast-wave fitting to the hadron spectra [8]. Figure 1 shows (left) the chemical freeze-out temperature, $T_{\rm ch}$ (MeV), with respect to the baryon chemical potential, $\mu_{\rm B}$ (MeV), and (right) kinetic freeze-out temperature, $T_{\rm kin}$ (MeV), with respect to the collective velocity, $\langle\beta\rangle$. It is found that $T_{\rm ch}$ is almost independent on the centrality, while $\mu_{\rm B}$ strongly depends on it. We see lower values of $T_{\rm kin}$ with larger $\langle\beta\rangle$ in central collisions, and the stronger collectivity seems to be realized at high energy even in the peripheral collisions. Comparing the chemical and kinetic freeze-out temperature, one immediately find that there is a large gap between $T_{\rm ch}$ and $T_{\rm kin}$ increasing with beam energy, which would indicate that the hadronic system interacts for longer duration in higher collision energies.

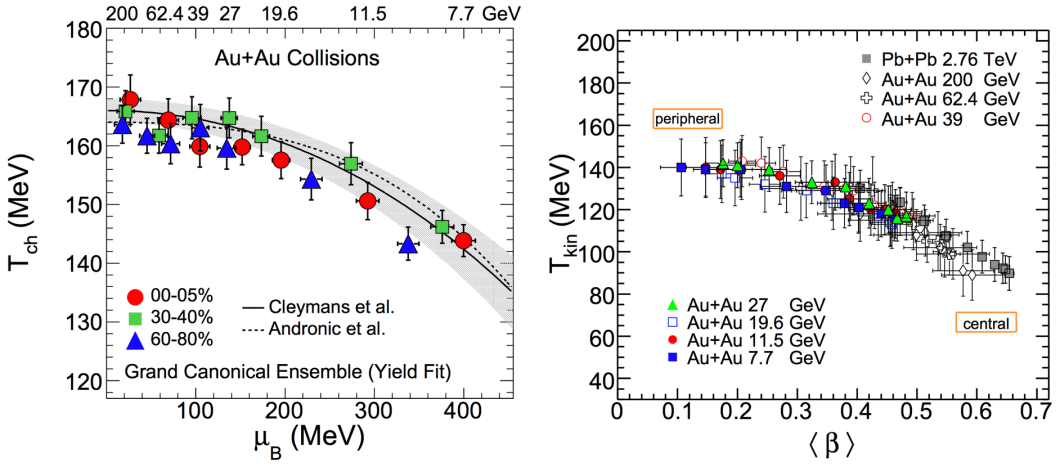

Fig. 1. (Left) The chemical freeze-out temperature, $T_{\rm ch}$, as a function of the baryon chemical potential, $\mu_{\rm B}$, in Au+Au collisions [4]. Colored markers and lines represent the STAR results and HRG model expectations [5, 6]. (Right) The kinetic freeze-out temperature, $T_{\rm kin}$, as a function of the collectivity $\langle\beta\rangle$ in Pb+Pb and Au+Au collisions [4].

3. Searching for the 1st-order phase transition

In order to find the signal of the 1st-order phase transition, the directed flow, v_1, of identified particles has been measured as a function of rapidity [9, 10]. Figure 2 shows the slope parameter, dv_1/dy, at $y = 0$ as a function of collision energy. It is found that the results for net proton and net Λ has a minimum around $\sqrt{s_{\rm NN}}$ = 14.5 and 20 GeV. This behaviour is qualitatively consistent with the theoretical prediction, where a dip in dv_1/dy is expected at around a collision energy due to softening of the equation of state in the vicinity of phase transition.

The experimental results do not show the softest point for mesons, but only for baryons. Model explanation is needed for further understanding of the experimental data.

4. Mapping the QCD phase diagram using higher-order cumulants

4.1 Fluctuations of conserved quantities

The higher-order fluctuations have been actively measured in the STAR experiment to study the QCD phase diagram. The higher-order fluctuations are characterized by the mth-order cumulants of the event-by-event number distribution of conserved quantities like net baryon, net charge and net

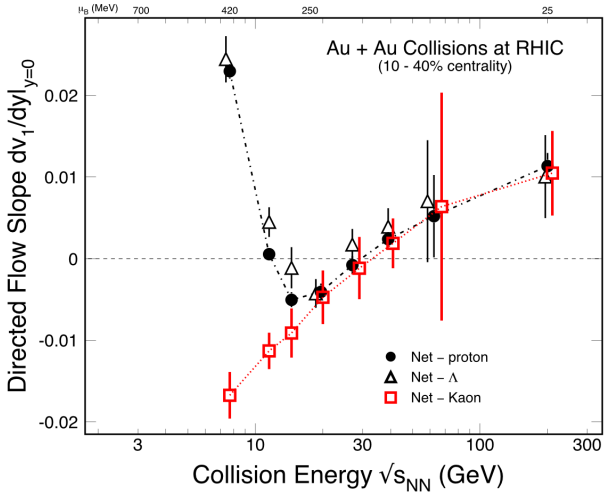

Fig. 2. The slope of the directed flow at $y = 0$ as a function of the collision energy in Au+Au collisions [9, 10]. Black points represent net-proton, black triangles represent net-Λ and red squares represent net-kaon.

strangeness. It is predicted that the higher the order of the cumulant is, the more sensitive it is to the correlation length [13]. The relation between the cumulants and correlation length are give as below;

$$C_2 \propto \xi^2,\ C_3 \propto \xi^{4.5},\ C_4 \propto \xi^7,\ C_5 \propto \xi^{9.5},\ C_6 \propto \xi^{12}. \tag{1}$$

Since the correlation length, ξ, is predicted to diverge at the vicinity of the critical point, a large increase is expected in the higher-order cumulants near the critical point. Cumulants have the volume dependence by definition. In order to remove the volume dependence, the higher-order cumulants normalized to the lower-order cumulants are usually calculated, for example:

$$C_2/C_1 = \sigma^2/M,\ C_3/C_2 = S\sigma,\ , C_4/C_2 = \kappa\sigma^2, \tag{2}$$

where the right hand side of the equations are the expressions using moments.

4.2 Data analysis method

In the data analysis, the following items need to be carefully taken into account; a) statistical error estimation, b) auto-correlation and centrality resolution effects, c) initial volume fluctuations, d) detector inefficiency. In the STAR experiment, the statistical uncertainty is estimated using the delta-theorem or bootstrap method. The auto-correlation and centrality resolution effects have been suppressed by defining the centrality using charged particles except protons and antiprotons. The effect from the initial volume fluctuations can be reduced by applying the centrality bin width averaging. The detector inefficiency is corrected by assuming that the efficiency follows the binomial distribution. These methods are well discussed in the literature [15–19].

4.3 Critical point search using the 4th-order fluctuation

The higher-order fluctuations were measured for the first time with respect to the net-proton multiplicity distributions at $\sqrt{s_{\rm NN}}$ =19.6, 62.4 and 200 GeV, where the 4th-order fluctuations were found to be flat at $\mu_{\rm B} < 210$ MeV [20,21]. Up to the 4-th order fluctuations were measured for the net-proton, net-charge and net-kaon multiplicity distributions in BES-I [22–24]. The minimum seemed to appear at $\sqrt{s_{\rm NN}} = 19.6$ GeV for 3rd- and 4th-order fluctuations of the net-proton distribution, but the effects were not significant enough. Afterward, it was found that the number of protons and antiprotons can be doubled by extending the p_T acceptance from $0.4 < p_T < 0.8$ GeV/c to $0.4 <$

p_T < 2.0 GeV/c, which was realized using TOF in addition to TPC for the particle identification. Figure 3 shows the results of the 4th-order fluctuations of net-proton multiplicity distribution with the extended p_T acceptance [25]. It is seen that the results for the central collisions show the minimum at $\sqrt{s_{\rm NN}}$ = 19.6 GeV, and show strong enhancement at lower collision energies, whose trend is in accord with a theoretical model prediction [14]. It is also to be noted that any model simulation shows the suppression of the 4th-order fluctuations of the net-proton distribution at $\sqrt{s_{\rm NN}} \leq 20$ GeV [26, 28, 31], which is mainly due to the baryon stopping effect. Therefore, this non-monotonic beam energy dependence of the 4th-order fluctuations could indicate a signal from the critical point. Since the uncertainties for low collision energies are large, the BES-II program will be carried out in 2019-2021 focusing on $\sqrt{s_{\rm NN}} \leq 19.6$ GeV to extract more definite physics messages.

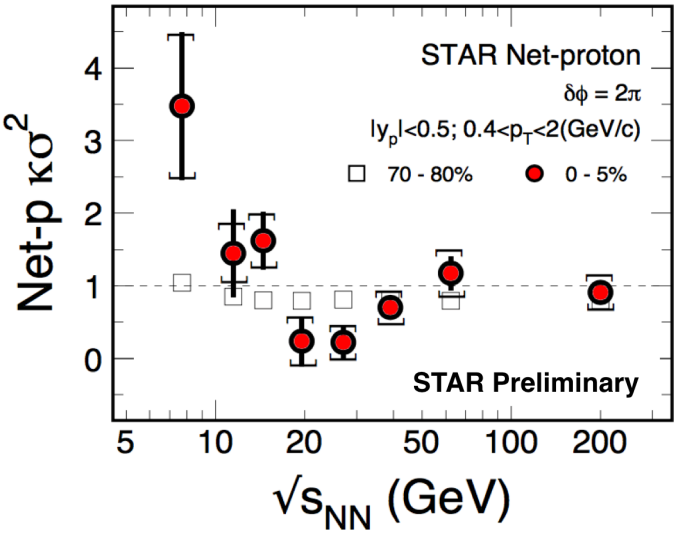

Fig. 3. The 4th-order fluctuations, $\kappa\sigma^4 = C_4/C_2$, of the net-proton multiplicity distributions as a function of collision energy. Red circles and open squares represent the data for 0–5% and 70–80% central collisions, respectively.

4.4 Crossover search using the 6th-order fluctuation

One should not forget that the crossover at $\mu_{\rm B} = 0$ MeV was shown only by the lattice QCD calculation [1], and there is not yet any experimental evidence for the crossover. Theoretically, the 6th-order fluctuations, C_6/C_2, are predicted to be sensitive to the crossover as well as the critical point. It is expected that C_6/C_2 becomes negative if the freeze-out temperature is close enough to the phase transition temperature at the beam energy of $\sqrt{s_{\rm NN}} \geq 60$ GeV [29]. Figure 4 shows C_6/C_2 as a function of centrality at $\sqrt{s_{\rm NN}}$ = 54.4 and 200 GeV. It was found that the $C_6/C_2 > 0$ at $\sqrt{s_{\rm NN}}$ = 54.4 GeV, while $C_6/C_2 < 0$ at $\sqrt{s_{\rm NN}}$ = 200 GeV in central collisions. This result is qualitatively consistent with the theoretical prediction, and it suggests the crossover transition at $\sqrt{s_{\rm NN}}$ = 200 GeV. In addition, the UrQMD results at $\sqrt{s_{\rm NN}}$ = 200 GeV show $C_6/C_2 > 0$ for all centralities, which indicates that $C_6/C_2 < 0$ cannot be realized by the hadron transport model. The experimental results can also be compared with the lattice QCD calculations as a proxy for $\mu_{\rm B} \sim 0$ MeV. Figure 4 shows that both results are consistent with each other in central collisions within large uncertainties.

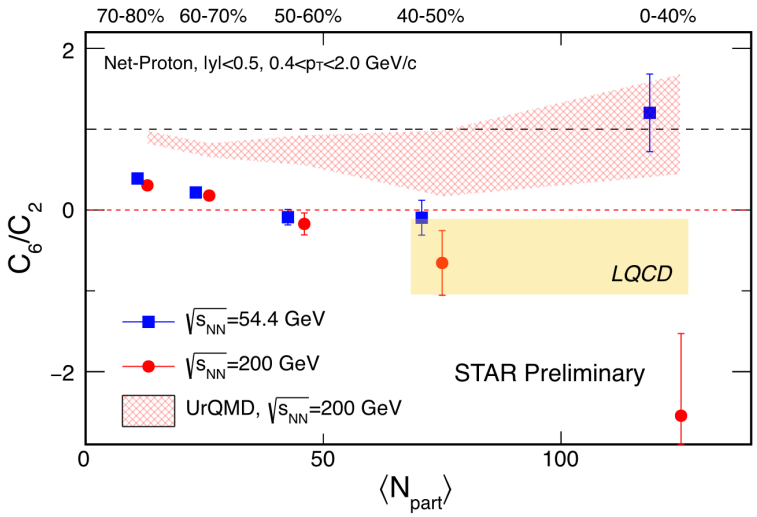

Fig. 4. The 6th-order fluctuations, C_6/C_2, of the net-proton multiplicity distributions at $\sqrt{s_{\rm NN}}$ = 54.4 and 200 GeV as a function of centrality. The red band represents UrQMD results at $\sqrt{s_{\rm NN}}$ = 200 GeV. The yellow band represents results of the lattice QCD calculation [30].

5. Beam Energy Scan Phase II

Many results in BES-I had large uncertainties at low beam energies due to limited statistics, which made it difficult to extract definitive physics messages. Thus, the beam energy scan program phase II (BES-II) will be carried out focusing on $\sqrt{s_{\rm NN}} \leq 19.6$ GeV in 2019-2021 , where 10-20 times larger statistics than in BES-I will be collected. The expected errors of the 4th-order fluctuations of the net-proton multiplicity distribution are shown as a green band at the right hand side of Fig. 5. After we confirm the significant enhancement of the 4th-order fluctuations at low beam energies with better precision in BES-II, the main point will be whether we see the predicted peak structure in further lower energies. This will be investigated by future experiments.

6. Summary

We presented experimental results related to the QCD phase structure obtained by STAR. The QCD phase diagram has been studied in the view of the freeze-out conditions, 1st-order phase transition, critical end point and crossover by measuring the hadron yields, spectra, directed flow of identified particles, and higher-order fluctuations of net-proton multiplicity distributions. Most importantly, non-monotonic beam energy dependence has been observed in the net-proton 4th-order fluctuations for 0–5% central collisions, which could be a signal from the critical point at low collision energies. In order to increase precision, the BES-II program will be carried out in 2019-2021 focusing on $\sqrt{s_{\rm NN}} \leq 19.6$ GeV and get more insights for the critical point.

7. Acknowledgement

This work is supported by the MoST of China 973-Project No. 2015CB856901, the National Natural Science Foundation of China under Grants (No. 11575069, 11828501, 11890711 and 11861131009), Fundamental Research Funds for the Central Universities NO. CCNU19QN054 and China Postdoctoral Science Foundation funded project 2018M642878.

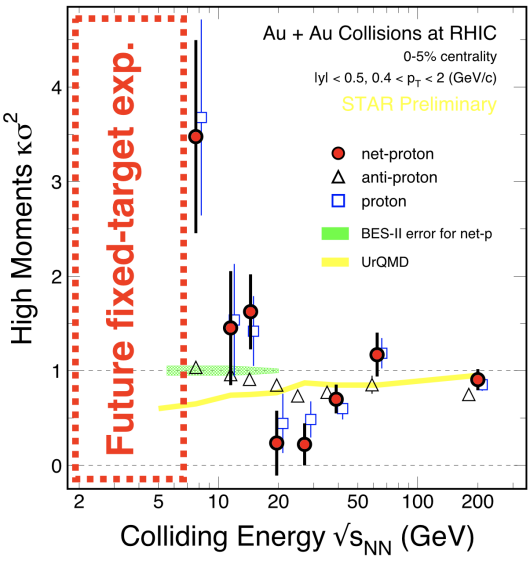

Fig. 5. The 4th-order fluctuations of the net-proton distribution as a function of beam energy in central collisions. The expected uncertainties for BES-II data are shown as a green band. The yellow band represents the results of the hadron transport model [31].

References

[1] Y. Aoki et al., Nature **443** (2006) 675-678
[2] C. M. Hung and E. V. Shuryak, Phys. Rev. Lett. **75** (1995) 4003
[3] D. H. Rischke et al., Acta Phys. Hung. **A1** (1995) 309-322
[4] L. Adamczyk et al. (STAR Collaboration), Phys. Rev. C **96** (2017) 044904
[5] J. Cleymans et al., Phys. Rev. C **73** (2006) 034905
[6] A. Andronic et al., Nucl. Phys. A **834** (2019) 237c
[7] S. Wheaton et al., Comput. Phys. Commun. **180** (2009) 84
[8] E. Schnedermann et al., Phys. Rev. C **48** (1993) 2462
[9] L. Adamczyk et al. (STAR Collaboration), Phys. Rev. Lett. **112** (2014) 162301
[10] L. Adamczyk et al. (STAR Collaboration), Phys. Rev. Lett. **120** (2018) 062301
[11] M. Isse et al., Phys. Rev. C **72** (2005) 064908
[12] Y. Nara et al., Phys. Rev. C **94** (2016) 034906
[13] M. A. Stephanov, Phys. Rev. Lett. **102** (2009) 032301
[14] M. A. Stephanov, Phys. Rev. Lett. **107** (2011) 052301
[15] X. Luo et al., J. Phys. G **40** (2013) 105104
[16] A. Bzdak and V. Koch, Phys. Rev. C **86** (2012) 044904
[17] X. Luo, Phys. Rev. C **91** (2015) 034907
[18] T. Nonaka et al., Phys. Rev. C **95** (2017) 064912
[19] X. Luo and T. Nonaka, arXiv:1812.10303
[20] M. M. Aggarwal et al. (STAR Collaboration), Phys. Rev. Lett. **105** (2010) 022302
[21] S. Gupta et al., Science **332** (2011) 1525-1528
[22] L. Adamczyk et al. (STAR Collaboration), Phys. Rev. Lett. **112** (2014) 032302
[23] L. Adamczyk et al. (STAR Collaboration), Phys. Rev. Lett. **113** (2014) 092301
[24] L. Adamczyk et al. (STAR Collaboration), Phys. Lett. B **785** (2018) 551
[25] X. Luo (STAR Collaboration), PoS CPOD2014 (2015) 019 [arXiv:1503.025558]
[26] Z. Feckova et al., Phys. Rev. C **92** (2015) 064908
[27] J. Xu et al., Phys. Rev. C **94** (2016) 024901
[28] S. He et al., Phys. Lett. B **762** (2017) 296
[29] B. Friman et al., Eur. Phys. J. C **71** (2011) 1694
[30] A. Bazavov et al., Phys. Rev. D **95** (2017) 054504
[31] J. Xu et al., Phys. Rev. C **94** (2016) 024901